2.4 Compact Mach-Zehnder acousto-optic modulator

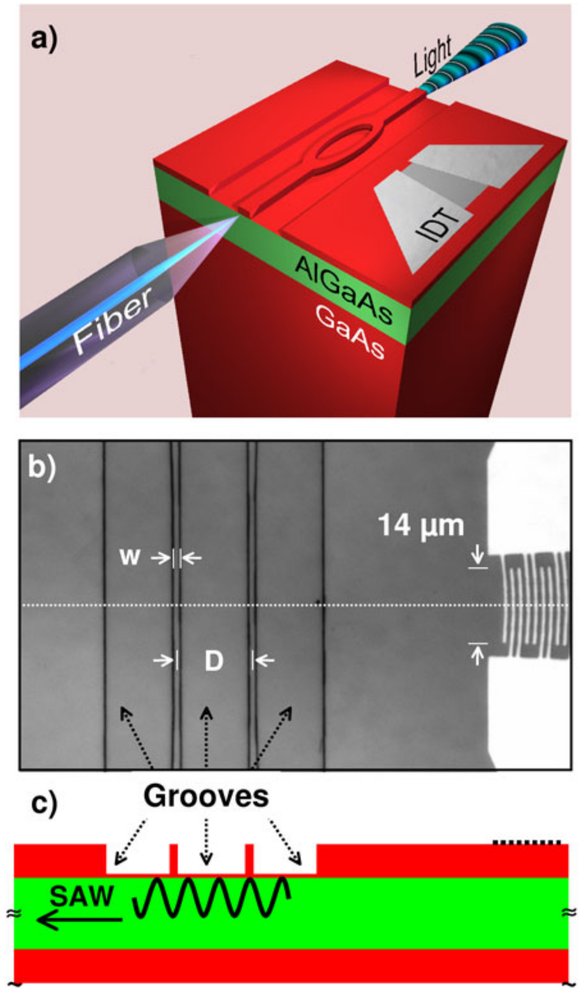

Fig. 10. (a) Schematic view of the MZI modulated by a SAW. The incoming light is coupled into the device by a tapered fiber while the modulated outgoing light is detected at the opposite cleaved edge. The SAW is generated by a focusing IDT. (b) Optical micrograph with a top view of the MZI active area. (c) Cross-sectional view of the ridge waveguides forming the MZI arms, which are spaced by $2.5\lambda_{SAW}$ to experience opposite phases of the acoustic field.

The control of light beams through acousto-optic interaction normally requires a phase matching between the electromagnetic and acoustic waves. This constraint severely limits the application of this effect for optical switching and modulation in planar waveguide (WG) structures. We demonstrate one approach to overcome this limitation using an acoustically driven Mach-Zehnder interferometer (MZI) monolithically fabricated on a GaAs substrate. The devices operate as compact modulators for the GHz frequency range.

The device illustrated in Fig. 10(a) is a MZI, where the arms are modulated by a surface acoustic wave (SAW). The SAW is excited by an interdigital transducer (IDT). The design employed by us is a modified version of an original proposal by C. Gorecki *et al.* [Opt. Lett. **22**, 1784 (1997)]. In our case, the SAW wavefronts modulate simultaneously the refractive index of both interferometer arms. For that purpose, the arms are separated by a distance D equal to an odd multiple of half of the acoustic wavelength λ_{SAW}, in order to experience refractive index changes of opposite phase during the passage of the SAW as shown in the top and cross-section views of Figs. 10(b) and 10(c), respectively. The width of the waveguides forming the arms was chosen to be much smaller than the acoustic wavelength in order to ensure a homogeneous modulation amplitude across the WG width. Finally, we used a SAW generated by a focusing IDT, which creates a narrow and strong acoustic beam. In this way, the length of the interaction region between the acoustic and electromagnetic waves (the active region) was reduced to approximately 15 μm.

The device operation is illustrated in the time-resolved transmission traces of Fig. 11, which were recorded for different rf-powers (P_{IDT}) coupled to the IDT. In these experiments, light with TE polarization was coupled into the WGs using a tapered optical fiber [cf. Fig. 10(a)] and the

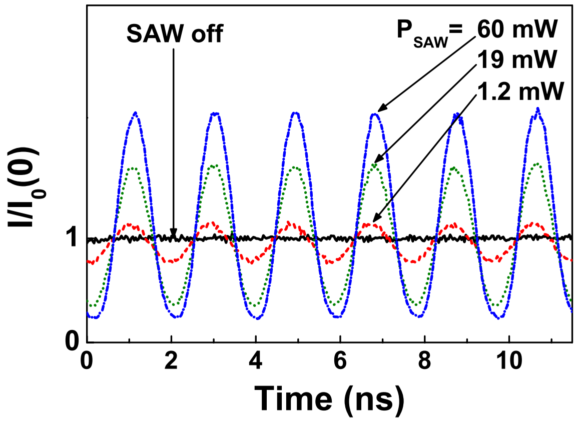

Fig. 11. Measured light transmission (I) through the MZI vs. time for different acoustic powers (P_{IDT}) applied to the IDT. The curves are normalized to the transmission in the absence of a SAW [$I_0(0)$].

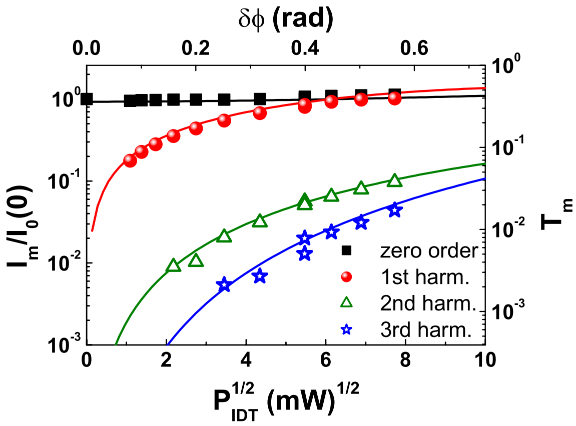

Fig. 12. Amplitude of the m^{th}-order harmonic of the transmitted intensity [$I_m(P_{\mathrm{IDT}})$] as a function of $\sqrt{P_{\mathrm{IDT}}}$ (symbols), normalized to $I_0(0)$. The solid lines correspond to results from calculations assuming a static phase shift between the arms equal to $\delta\phi_s = 0.927$ rad.

transmitted light was detected using an avalanche photodiode. Oscillations of the transmitted intensity with the SAW period and with an amplitude increasing with P_{IDT} were observed. For the highest acoustic power ($P_{\mathrm{IDT}} = 60$ mW), the modulation amplitude became comparable to the average transmission in the absence of acoustic excitation. The oscillations were asymmetric in this case, thus indicating the presence of higher harmonics. The distribution of harmonics as extracted from the Fourier transform of the transmission data are displayed in Fig. 12. Here, the transmission intensity (I_m) modulated at the m^{th} harmonic of the SAW frequency was normalized to the intensity $I_0(0)$ in the absence of acoustic excitation. Transmission up to the third harmonic of the SAW frequency was clearly observed. The detection of higher harmonics (with frequencies >2 GHz) is beyond the time resolution of the experimental setup. In agreement with the previous discussion, the amplitude of the first harmonic T_1 approaches 90% of the continuous transmission T_0 for $P_{\mathrm{IDT}} = 60$ mW. The lines in the diagram are fits to the transmission function of the acoustic MZI, which take into account the absolute refractive index modulation by the SAW. The fits are in excellent agreement with the experiment and yield a static light phase shift $\delta\phi_s = 0.927$ rad between the arms.

In summary, we demonstrated an acoustically-driven compact waveguide modulator based on a MZI driven by a surface acoustic wave. Peak-to-peak modulation amplitudes exceeding 90% were achieved together with modulation up to the third harmonic at 1.56 GHz. The modulation concept described here can easily be extended to silicon-based optoelectronic components by depositing a piezoelectric overlayer on the substrate.

(M. M. de Lima, Jr., M. Beck, R. Hey, P. V. Santos)